THERMOELASTIC STRESSES IN FUNCTIONALLY GRADED ROTATING ANNULAR DISKS WITH VARIABLE THICKNESS

MOHAMMED N.M. ALLAM

Mansoura University, Faculty of Science, Department of Mathematics, Mansoura

RANIA TANTAWY

Damietta University, Faculty of Science, Department of Mathematics, Damietta, Egypt

ASHRAF M. ZENKOUR

King Abdulaziz University, Faculty of Science, Department of Mathematics, Jeddah, Saudi Arabia, and

Kafrelsheikh University, Faculty of Science, Department of Mathematics, Kafrelsheikh, Egypt

e-mail: zenkour@kau.edu.sa; zenkour@kaf-sci.edu.eg

This article presents semi-analytical solutions for stress distributions in exponentially and functionally graded rotating annular disks with arbitrary thickness variations. The disk is under pressure on its boundary surfaces and exposed to temperature distribution varying linearly across thickness. Material properties are supposed to be graded in the radial direction of the disk and obeying to two different forms of distribution of volume fraction of constituents. Different conditions at boundaries for stresses and displacement are discussed. Accurate and efficient solutions for displacement and stresses in rotating annular disks are determined using infinitesimal theory. Numerical results are carried out and discussed for different cases. It can be deduced that the gradient of material properties and thickness variation as well as the change of temperature sources have a specific effect in modern applications.

Keywords: functionally graded, variable thickness, semi-analytical approach, rotating, thermal effect

1. Introduction

Stress analyses of rotating circular disks have long been an important topic in engineering applications. Disks made of homogeneous materials have been discussed extensively with constant and thickness variation (Hartog, 1952). Cavallaro (1965) presented variable-thickness disks, symmetrical with respect to both their axes and their mid-planes, under the effect of centrifugal and thermal loadings. Wu and Ramsey (1966) presented solutions for stresses in rotating, symmetrical, three-layer circular disks. Murthy and Sherbourne (1970) presented rotating anisotropic variable-thickness disks under centrifugal loading. Yella Reddy and Srinath (1974) derived closed-form solutions for the bending response of rotating variable-thickness and variable-density disks. Sherbourne and Murthy (1974) presented a dynamic relaxation technique to study stresses and displacements of rotating variable-thickness disks with different boundary conditions.

An extension to rotating solid and annular disks with variable profiles made of viscoelastic materials has been investigated. Feng (1985) presented governing equations of rotating disks subjected to large elastic and viscoelastic deformations. Allam *et al.* (2008) presented a circular variable-thickness elastic disk under the effect of steady coaxial current and bearing coaxial viscoelastic coating. Zenkour and Allam (2006) presented an analytical solution for displacement and stresses in rotating fiber-reinforced viscoelastic variable-thickness disks. Allam *et al.* (2007) presented analytical solutions for inhomogeneous rotating variable-thickness viscoelastic disks.

Recently, the research on rotating circular disks has become more and more active after changing the material model, especially in the case of functionally graded materials (FGMs) (Argeso, 2012; Das *et al.*, 2012; Hassani *et al.*, 2012; Peng and Li, 2012a,b; Golmakani, 2013; Kadkhodayan and Golmakani, 2014; Zenkour, 2014; Dai and Dai, 2015; Leu and Chien, 2015; Sahni and Sahni, 2015; Hosseini *et al.*, 2016; Zhenga *et al.*, 2016; Entezari *et al.*, 2017; Essa and Argeso, 2017; Tutuncu and Temel, 2013). Allam and Zenkour (2005) presented viscoelastic rotating disks of made of an exponentially graded (EG) varying thickness and fiber-reinforced viscoelastic material. Zenkour (2005) obtained accurate elastic solutions for EG rotating annular disks with different conditions. You *et al.* (2007) obtained closed-form solutions of FG rotating circular disks under uniform angular velocity and uniform temperature change taking into consideration that material properties were functions of the radial coordinate. Bayat *et al.* (2008), Asghari and Ghafoori (2010) and Ghorbanpour Arani *et al.* (2010) used a semi-analytical method to present elastic and magneto-thermo-elastic solutions for FG rotating disks with a variable profile. Vullo and Vivio (2008) obtained elastic stresses and strains in rotating variable-thickness solid and annular disks under thermal load with density variation along the radial coordinate. Bayat *et al.* (2009a,b) used the first-order shear deformation theory to discuss elastic and thermoelastic bending responses of rotating disks with graded material properties. Bayat *et al.* (2009c) derived thermoelastic responses for axisymmetric FG rotating variable-thickness disks with temperature--dependent material properties. Zenkour (2009) presented two models of sandwich rotating solid disks with the EG core with free or clamped-edge conditions. The finite difference, finite element and semi-exact elastic solutions of thermoelastic analysis of FG rotating disks were presented by Afsar and Go (2010), Hassani *et al.* (2011), Sharma (2013), Zafarmand and Hassani (2014), Arnab *et al.* (2014), and Entezari *et al.* (2017).

An additional extension to thermo-piezo-magneto-mechanical stresses analyses of FG rotating disks was presented by Ghorbanpour Arani (2010a, b). Dai *et al.* (2017) presented temperature, moisture, displacement and stress distributions of an exponentially graded piezoelectric (EGP) rotating disk. Dai and Dai (2017) presented a rotating disk with variable thickness in thermal environment made of an FG magneto-electro-elastic material (MEEM). In this article, the problem of stresses and deformation of a rotating variable-thickness inhomogeneous and FG annular disk is presented. Numerical results are investigated according to different profiles of the annular disk. Two specific thickness variations namely power and exponential laws for thickness variation are considered. A comparison between different cases is made and some conclusions are presented.

2. Formulation of the problem

Here, the basic equations of elasticity are used (Mashat and Zenkour, 2014). The constitutive equations are represented as

$$
\sigma_r = \frac{E}{1-\nu^2}\Big(\nu\frac{u}{r} + \frac{du}{dr}\Big) - \frac{E}{1-\nu}\alpha T
$$
$$
\sigma_\theta = \frac{E}{1-\nu^2}\Big(\frac{u}{r} + \nu\frac{du}{dr}\Big) - \frac{E}{1-\nu}\alpha T
$$

(2.1)

where u represents the radial displacement, σ_r and σ_θ denote radial and hoop stresses, T is temperature distribution, E denotes Young's modulus, ν denotes Poisson's ratio and α represents the thermal expansion coefficient. It is considered that thickness is a function of the radial coordinate, that is $h(r)$ represents variable-thickness of the rotating disk. So, the dynamic equation of a rotating variable-thickness disk may be represented by

$$
\frac{d}{dr}(hr\sigma_r) - h\sigma_\theta + h\rho\omega^2 r^2 = 0
$$

(2.2)

where ω represents angular velocity and ρ denotes material density. Assume that the material of the rotating disk is isotropic with uniform Poisson's ratio while the elastic modulus, density, and thermal coefficient are all radially varying. Equation (2.2) with the help of Eq. (2.1) yields

$$\frac{d^2u}{dr^2} + \left(\frac{1}{r} + \frac{1}{E}\frac{dE}{dr} + \frac{1}{h}\frac{dh}{dr}\right)\frac{du}{dr} + \left[\frac{\nu}{r}\left(\frac{1}{E}\frac{dE}{dr} + \frac{1}{h}\frac{dh}{dr}\right) - \frac{1}{r^2}\right]u$$
$$+ (\nu + 1)\left[\frac{\omega^2\rho r}{E}(1-\nu) - \alpha\frac{dT}{dr} + \left(\frac{d\alpha}{dr} + \alpha\frac{1}{E}\frac{dE}{dr} + \alpha\frac{1}{h}\frac{dh}{dr}\right)T\right] = 0 \qquad (2.3)$$

3. Various disk profiles

3.1. Thickness profiles

The present rotating disk is annular and made of a variable-thickness, single-layer of functionally or exponentially graded material with the inner radius a and the outer one b. Two thickness disk profiles are supposed here. In the first one, the thickness is varied with radius of the disk according to the following power-law form

$$h(r) = h_0\left[1 - n\left(\frac{r}{b}\right)\right]^k \qquad (3.1)$$

where h_0 denotes the thickness at the axis of the disk and n and k are dimensionless parameters. The parameter n defines thickness at edge of the disk relative to h_0 while the parameter k defines the shape of the disk profile. The uniform-thickness disk is deduced when either $n = 0$ or $k = 0$ while linearly-decreasing thickness is deduced if $k = 1$. In addition, if $k < 1$ the disk profile is convex while if $k > 1$ it is concave. Figure 1 illustrates the case of a convex disk with $n = 0.415196$ and $k = 3$. The dimensionless thickness $\overline{h} = h(r)/h_0$ is displayed in terms of dimensionless radius $\overline{r} = r/b$ for $a = 0.2\,\text{m}$.
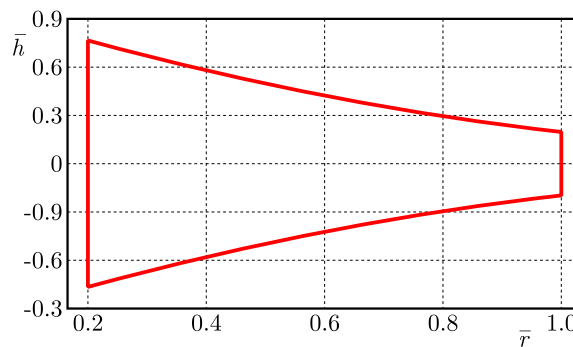

Fig. 1. Power disk profiles, $n = 0.415196$ and $k = 3$

The second thickness of the disk profile is considered to vary radially according to this exponential form

$$h(r) = h_0\exp\left[-n\left(\frac{r}{b}\right)^k\right] \qquad (3.2)$$

Also, in this case n defines thickness at edge of the disk and k determines the shape of the disk profile. Figure 2 shows two plots of this disk profile in two cases: (a) $n = 2$ and $k = 0.5$ while (b) $n = 0.415196$ and $k = 3$ for the same inner radius a.
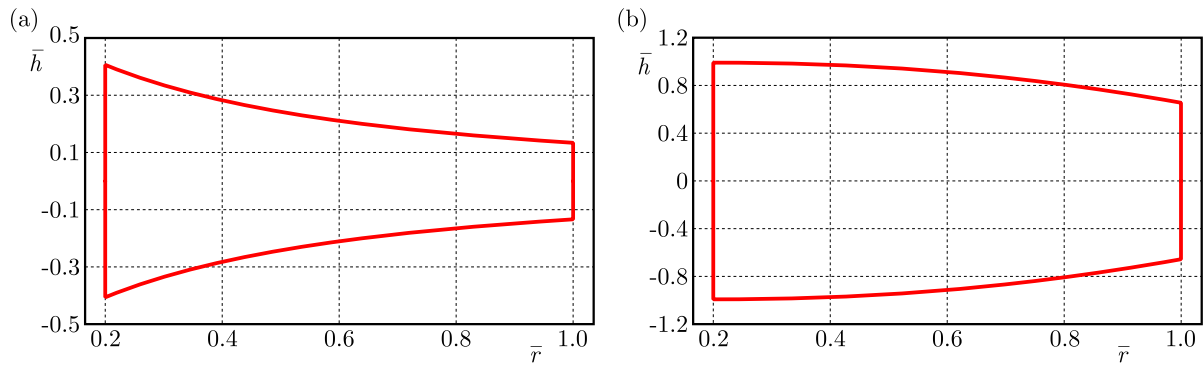
Fig. 2. Exponential disk profiles: (a) $n = 2$, $k = 0.5$, (b) $n = 0.415196$, $k = 3$

3.2. Material properties profiles

The material properties of the annular disk are considered to vary across the radial direction. Young's modulus E, thermal expansion coefficient α, and material density ρ are assumed to vary according to the following simple power law

$$P(r) = P_0\Big(\frac{r}{b}\Big)^{\beta} \tag{3.3}$$

where P_0 is the material property (E_0, α_0 and ρ_0) at the outer surface of the disk and β denotes the inhomogeneity parameter. The above formula means that the annular disk is inhomogeneous with respect to its coefficients ρ, α, and E.

For the functionally graded (FG) annular disk, the property variation $P(r)$ of the thermal coefficient, density and modulus of elasticity across the radial direction is considered as (Ruhi *et al.*, 2005)

$$P(r) = P_a + (P_b - P_a)\Big(\frac{r - a}{b - a}\Big)^{\beta} \tag{3.4}$$

where P_a and P_b denote the corresponding properties of the inner and outer surfaces of the rotating disk. The grading index parameter $\beta \geqslant 0$ represents the volume fraction exponent. The above power law reflects a simple rule of mixture in terms of volume fraction of constituents, and it is widely admitted form of property variation.

3.3. Temperature profiles

The temperature distribution across the radial direction is derived from heat conduction equation

$$\kappa \nabla^2 T(r) + q(r) = 0 \tag{3.5}$$

where $\nabla^2 = (d^2/dr^2) + (1/r)(d/dr)$, κ denotes thermal conductivity, and q represents the heat generation function. The temperature satisfies the following boundary conditions

$$T(r)\big|_{r=a} = T_0 \qquad \frac{dT(r)}{dr}\Big|_{r=b} = 0 \tag{3.6}$$

in which T_0 denotes the reference temperature. The internal energy generation within both surfaces is given by the heat generating function

$$q(r) = -Q\Big(\frac{r - a}{a}\Big)\Big(\frac{r - b}{b}\Big) \qquad a \leqslant r \leqslant b \tag{3.7}$$

where Q represents a uniform rate of internal energy generation. So, Eq. (3.5) gets the solution

$$T(r) = \frac{Qr^2}{144\kappa ab}[9(r^2 + 4ab) - 16r(a + b)] + c_1 \ln(r) + c_2 \tag{3.8}$$

in which c_1 and c_2 represent arbitrary integration constants obtained from conditions appeared in Eq. (3.6) as

$$
\begin{aligned}
c_1 &= \frac{Qb^2}{12\kappa a}(b - 2a) \\
c_2 &= \frac{Q}{144\kappa ab}[a^3(7a - 20b) - 12b^3 \ln(a)(b - 2a)] + T_0
\end{aligned}
\tag{3.9}
$$

In addition to Eq. (3.8), one can use another simple and efficient form of temperature. That is

$$T(r) = T_a + \frac{T_b - T_a}{\ln \frac{b}{a}}(\ln r - \ln a) \tag{3.10}$$

4. Solution of the problem

It is known that it is difficult to get a general solution of the second-order differential equation with variable coefficients as Eq. (2.3). A semi-analytical approach is presented here for this purpose. The radial domain will be divided into some virtual sub-domains with thickness $s^{(m)}$ as illustrated in Fig. 3. Evaluating the coefficients of Eq. (2.3) at $r = r^{(m)}$, which is said to be
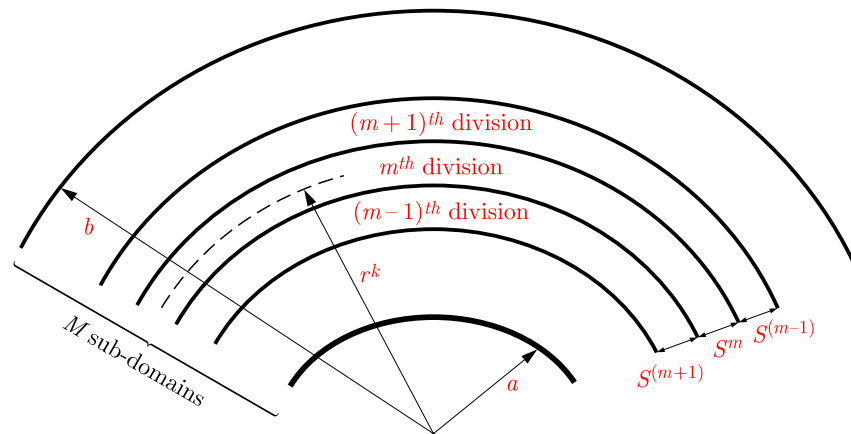

Fig. 3. Dividing radial domain into some finite sub-domains

the mean radius of m-th division, and using them instead of variable coefficients one obtains

$$\frac{d^2u^{(m)}}{dr^2} + N_1^{(m)}\frac{du^{(m)}}{dr} + N_2^{(m)}u^{(m)} - N_3^{(m)} = 0 \tag{4.1}$$

where

$$N_1^{(m)} = \frac{1}{r^{(m)}} + \frac{1}{E(r^{(m)})}\frac{dE}{dr}\Big|_{r=r^{(m)}} + \frac{1}{h(r^{(m)})}\frac{dh}{dr}\Big|_{r=r^{(m)}}$$

$$N_2^{(m)} = \frac{\nu}{r^{(m)}}\left(\frac{1}{E(r^{(m)})}\frac{dE}{dr}\Big|_{r=r^{(m)}} + \frac{1}{h(r^{(m)})}\frac{dh}{dr}\Big|_{r=r^{(m)}}\right) - \frac{1}{(r^{(m)})^2}$$

$$N_3^{(m)} = (\nu + 1)\left[\frac{\omega^2 \rho(r^{(m)})r^{(m)}}{E(r^{(m)})}(\nu - 1) + \alpha(r^{(m)})\frac{dT}{dr}\Big|_{r=r^{(m)}}\right.$$

$$\left. + \left(\frac{d\alpha}{dr}\Big|_{r=r^{(m)}} + \frac{\alpha(r^{(m)})}{E(r^{(m)})}\frac{dE}{dr}\Big|_{r=r^{(m)}} + \frac{\alpha(r^{(m)})}{h(r^{(m)})}\frac{dh}{dr}\Big|_{r=r^{(m)}}\right)T(r^{(m)})\right] \tag{4.2}$$

Now, Eq. (4.1) becomes a system of M-equations. So, it is easy to obtain the solution of Eq. (4.1) as

$$u^{(m)} = B_1^{(m)}e^{\beta_1 r} + B_2^{(m)}e^{\beta_2 r} + \frac{N_3^{(m)}}{N_2^{(m)}} \tag{4.3}$$

where m represents the number of virtual sub-domains, and β_1 and β_2 denote roots of $\beta^2 + N_1^{(m)}\beta + N_2^{(m)} = 0$, and $B_1^{(m)}$ and $B_2^{(m)}$ denote uncharted constants for the m-th sub--domain. Indeed, the above solution is valid for

$$r^{(m)} - \frac{s^{(m)}}{2} \leqslant r \leqslant r^{(m)} + \frac{s^{(m)}}{2} \tag{4.4}$$

where $r^{(m)}$ and $s^{(m)}$ represent the mean radius and radial width of m-th sub-domain, respectively. The uncharted $B_1^{(m)}$ and $B_2^{(m)}$ can be derived by applying necessary conditions between each two adjacent sub-domains. The continuity conditions at the interfaces may be expressed as

$$u^{(m)}\Big|_{r=r^{(m)}+\frac{S^{(m)}}{2}} = u^{(m+1)}\Big|_{r=r^{(m+1)}-\frac{S^{(m+1)}}{2}}$$

$$\sigma_r^{(m)}\Big|_{r=r^{(m)}+\frac{S^{(m)}}{2}} = \sigma_r^{(m+1)}\Big|_{r=r^{(m+1)}-\frac{S^{(m+1)}}{2}} \tag{4.5}$$

The continuity and boundary conditions yield a set of linear algebraic equations in $B_1^{(m)}$ and $B_2^{(m)}$ ($m = 1, 2, \ldots, M$). After getting $B_1^{(m)}$ and $B_2^{(m)}$ and using them in Eqs. (4.3), $u^{(m)}$ are completely determined. The accuracy of the results improves if the number of divisions is increasing.

5. Numerical results and discussion

Many examples for the analysis of inhomogeneous or FG rotating annular disks are illustrated to discuss radial and hoop stresses, temperature and radial displacement. The following non--dimensional variables are fixed through numerical examples

$$\{\overline{r}, \overline{u}\} = \frac{1}{b}\{r, u\} \qquad \overline{T} = \frac{T}{T_0} \tag{5.1}$$

while other non-dimensional forms of stresses will be given according to the case studied. Now, we will discuss four examples to cover all the presented cases. In all cases studied, one can use some values for the parameters as $a = 0.2\,\mathrm{m}$, $b = 1\,\mathrm{m}$, and $\omega = 100\,\mathrm{s}^{-1}$.

5.1.   Example 1

In this case, thickness, material properties, and temperature profiles are given according to Eqs. (3.1), (3.3) and (3.10), respectively. For the thickness profile, the geometric parameters are given by $n = 0.415196$ and $k = 3$. The mechanical boundary conditions are represented as

$$u\big|_{r=a} = 0 \qquad \sigma_r\big|_{r=b} = -p \tag{5.2}$$

where p is the outer pressure. In this case, the dimensionless stresses are given by

$$\overline{\sigma}_i = \frac{\sigma_i}{p} \qquad i = r, \theta \tag{5.3}$$

The elastic and thermal constants are assumed as: $E_0 = 390\,\text{GNm}^{-2}$, $\rho_0 = 3.9\,\text{Mgm}^{-3}$, $\nu = 0.25$, $\alpha_0 = 7 \cdot 10^{-6}\,\text{K}^{-1}$, $T_a = 373\,\text{K}$, $T_b = 273\,\text{K}$.
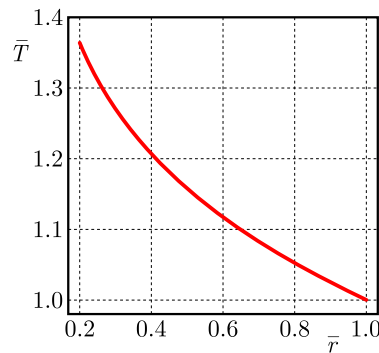

Fig. 4. Temperature distribution in an inhomogeneous rotating annular disk

The distribution of temperature is given in Fig. 4. The temperature, as expected, decreases as the radial direction increases. The radial stress $\overline{\sigma}_r$, hoop stress $\overline{\sigma}_\theta$ and radial displacement $\overline{u}$ are plotted in Figs. 5a,b,c. Different values of the inhomogeneity parameter β are considered. Figure 5a shows that $\overline{\sigma}_r$ for different values of β at $\overline{r} = 1$ is equal to -1, which satisfies the second part of conditions appeared in Eq. (5.2). The radial stress $\overline{\sigma}_r$ increases as β decreases while it is decreasing along the radial direction. Figure 5b plots the hoop stress $\overline{\sigma}_\theta$ across the radial direction
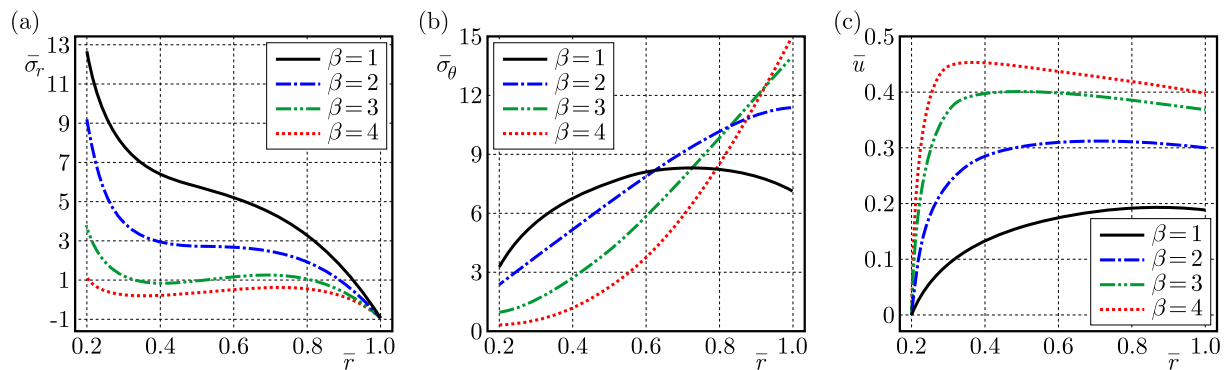

Fig. 5. (a) Radial stress, (b) hoop stress and (c) radial displacement distribution of the inhomogeneous rotating annular disk for different values of β

of the inhomogeneous annular disk. It is directly increasing to obtain its absolute maximum at the outer edge of the disk except for $\beta = 1$. The value of $\beta = 4$ yields the smallest hoop stress at the inner edge and greatest one at the outer edge. However, the value of $\beta = 1$ yields the greatest hoop stress at the inner surface and the smallest one at the outer surface. Figure 5c plots the

radial displacement distribution along the radial direction of the inhomogeneous annular disk. The radial displacement $\overline{u}$ for different values of β at $\overline{r} = 0.2$ is equal to zero, which satisfies the first part of the boundary conditions given in Eq. (5.2). The radial displacement $\overline{u}$ increases along the radial direction. Its maximum occurs at the outer edge for $\beta = 1$ only. However, this position of its maximum may be moved to be nearer to the inner surface as β increases.

5.2. Example 2

Here, thickness, material properties, and temperature profiles are given according to Eqs. (3.2), (3.3) and (3.10), respectively. The geometric parameters are taken as $n = 0.415196$ and $k = 3$. However, the mechanical conditions at boundaries are represented as

$$\sigma_r\big|_{r=a} = -p \qquad \sigma_r\big|_{r=b} = 0 \tag{5.4}$$

The results for such an inhomogeneous disk are illustrated in Figs. 6a,b,c. The non-dimensional forms for radial and hoop stresses appeared in Eq. (5.3) are repeated here. Figure 6a shows that $\overline{\sigma}_r$ for different values of β at $\overline{r} = 0.2$ is equal to -1 and at $\overline{r} = 1$ is equal to 0 according to conditions in Eq. (5.4). The differences between radial stresses $\overline{\sigma}_r$ increase at $r/b = 0.5$ with the occurrence of the absolute maximum value of $\overline{\sigma}_r$. Figure 6b shows that $\overline{\sigma}_\theta$ is directly increasing to get its absolute maximum at the outer surface of the inhomogeneous disk, except for $\beta = 1$. The value of $\beta = 4$ yields the smallest hoop stress at the inner edge and the greatest hoop stress at the outer edge. However, $\beta = 1$ yields the greatest hoop stress at the outer edge and the smallest hoop stress at the outer surface of disk. Figure 6c shows that $\overline{u}$ is decreasing to assume its absolute minimum at the outer edge for $\beta > 1$. However, it increases to get its absolute maximum at outer edge of the inhomogeneous disk.
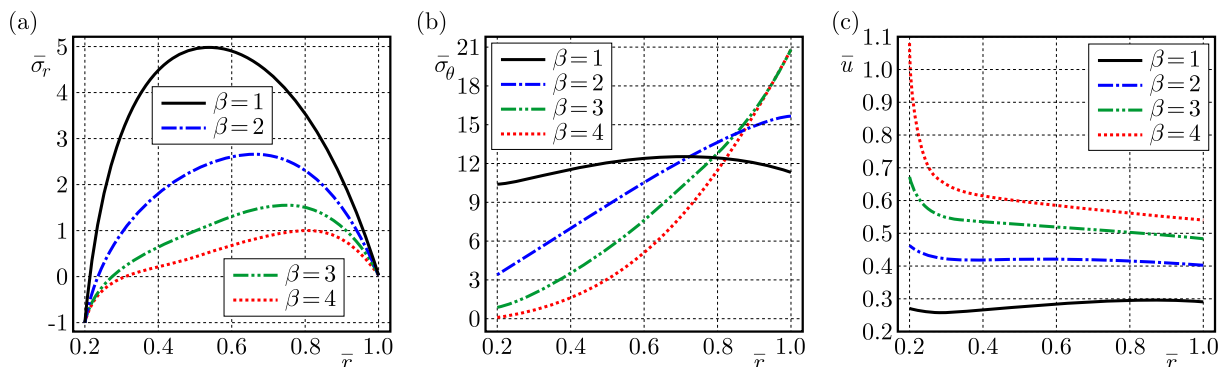

Fig. 6. (a) Radial stress, (b) hoop stress and (c) radial displacement distribution in the inhomogeneous rotating annular disk for different values of β

5.3. Example 3

The inner surface of the FG rotating annular disk is traction free while the outer one is under constant pressure. The mechanical boundary conditions are given in the form

$$\sigma_r\big|_{r=a} = 0 \qquad \sigma_r\big|_{r=b} = -p \tag{5.5}$$

where p is the outer pressure. The dimensionless stresses are also given as in Eq. (5.3). The thickness profile is given according to Eq. (3.2) with geometric parameters $n = 2$ and $k = 0.5$. The material properties profile is given according to Eq. (3.4) with $\nu = 0.3$ and $E_a = 390\,\text{GNm}^{-2}$, $E_b = 200\,\text{GNm}^{-2}$, $\rho_a = 3.9\,\text{Mgm}^{-3}$, $\rho_b = 7.7\,\text{Mgm}^{-3}$, $\alpha_a = 7 \cdot 10^{-6}\,\text{K}^{-1}$, $\alpha_b = 11 \cdot 10^{-6}\,\text{K}^{-1}$. The temperature profile is also given according to Eq. (3.10) with $T_a = 373\,\text{K}$ and $T_b = 273\,\text{K}$. The stresses and radial displacement are illustrated in Figs. 7a,b,c. From these figures, all stresses

and displacement increase with the decrease of the gradient parameter β. Figure 7a plots the radial stress distribution along the radial direction of the FG rotating disk. It is shown that $\overline{\sigma}_r$ for various values of β at $\overline{r} = 0.2$ is equal to 0 and at $\overline{r} = 1$ is equal to -1 according to conditions presented in Eq. (5.5). The differences between radial stresses $\overline{\sigma}_r$ increase near to the middle plane (far from internal and external boundaries). Figure 7b plots hoop stress $\overline{\sigma}_\theta$ along the radial direction. It is directly decreasing from its absolute maximum at the inner edge to get its absolute minimum at outer edge of the disk. Figure 7c shows that $\overline{u}$ is no longer decreasing and has its absolute minimum near the inner surface of the disk. Then, the radial displacement $\overline{u}$ is directly increasing to get its absolute maximum near the outer edge of the FG rotating annular disk.
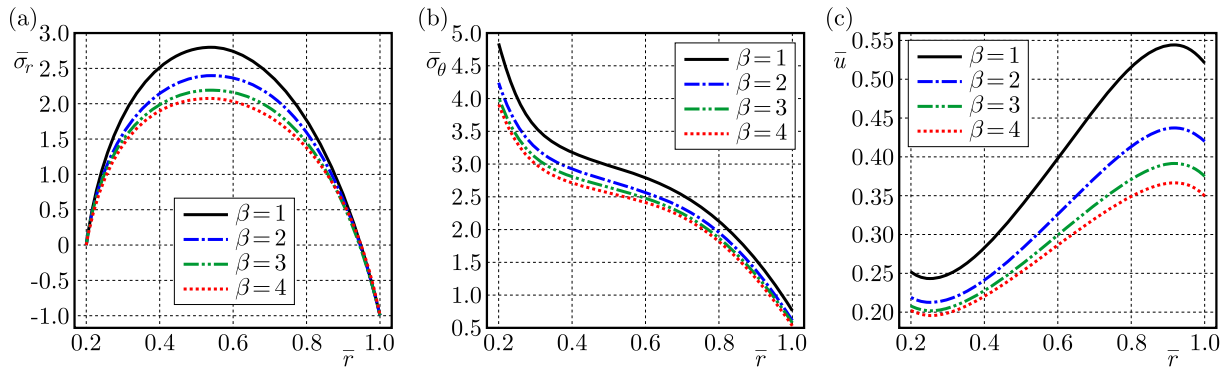

Fig. 7. (a) Radial stress, (b) hoop stress and (c) radial displacement distribution in the FG rotating annular disk for different values of β

5.4. Example 4

In this case, we take the same assumption of Example 3 except for temperature. It is given according to Eq. (3.8) with the help of Eq. (3.9). The uniform rate of internal energy generation Q, the thermal conductivity κ and the reference initial temperature T_0 are given, respectively, by $Q = 12\,\mathrm{W m^{-3}}$, $\kappa = 0.35\,\mathrm{W(Km)^{-1}}$, $T_a = 273\,\mathrm{K}$.

The mechanical boundary conditions are given by

$$\sigma_r\big|_{r=a} = -p_1 \qquad \sigma_r\big|_{r=b} = -p_2 \tag{5.6}$$

where p_2 and $p_1 = 0.6p_2$ are outer and inner pressures, respectively. The dimensionless stresses are given by

$$\overline{\sigma}_i = \frac{\sigma_i}{p_2} \qquad i = r, \theta \tag{5.7}$$

The dimensionless temperature distribution is plotted in Fig. 8. In addition, the radial and hoop stresses and radial displacement are illustrated in Figs. 9a,b,c. Figure 9a shows the radial stress distribution along the radial direction of the FG rotating disk. It is obvious that $\overline{\sigma}_r$ for various values of β at $\overline{r} = 0.2$ is equal to -0.6 and at $\overline{r} = 1$ is equal to -1, according to the conditions in Eq. (5.6). The radial stress $\overline{\sigma}_r$ has its absolute maximum value near the middle plane (far from internal and external boundaries). Figure 9b plots hoop stress $\overline{\sigma}_\theta$ along the radial direction. It is directly decreasing from its absolute maximum at the inner edge to get its absolute minimum at the outer edge of the disk. Figure 9c shows that $\overline{u}$ is no longer decreasing and has its absolute minimum near the inner edge of the disk. Then, it is directly increasing to get its absolute maximum near the outer surface. It is to be noted that all stresses and displacement increase as the gradient parameter β decreases.
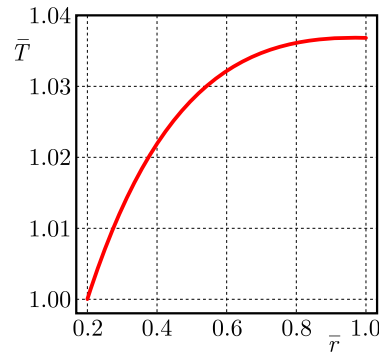
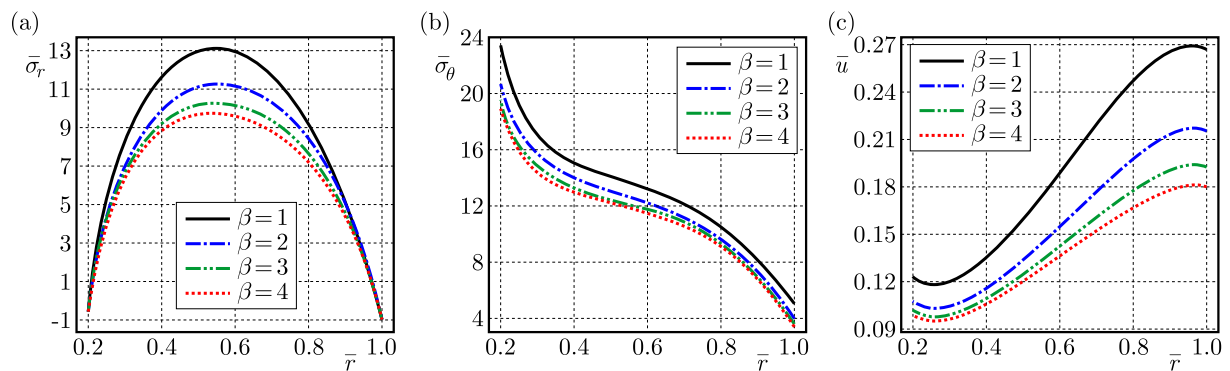Fig. 8. Temperature distribution in the FG rotating annular disk

Fig. 9. (a) Radial stress, (b) hoop stress and (c) radial displacement distribution in the FG rotating annular disk for different values of β

6. Concluding remarks

- In this article, semi-analytical solutions for stress distributions in inhomogeneous and FG variable-thickness rotating annular disks are investigated.
- The semi-analytical method is improved for the thermomechanical problem where stresses are produced based on different mechanical loading conditions.
- A selection of proper values of the graded index β and suitable loads helps engineers to design FG rotating disks that can meet some special requirements.
- The main conclusion is that the semi-analytical solution is an accurate and reliable, and the method is simple and effective.

References

1. AFSAR A.M., GO J., 2010, Finite element analysis of thermoelastic field in a rotating FGM circular disk, *Applied Mathematical Modelling*, **34**, 3309-3320

2. ALLAM M.N.M., BADR R.E., TANTAWY R., 2008, Stresses of a rotating circular disk of variable thickness carrying a current and bearing a coaxial viscoelastic coating, *Applied Mathematical Modelling*, **32**, 1643-1656

3. ALLAM M.N.M., ZENKOUR A.M., 2005, On the rotating fiber-reinforced viscoelastic composite solid and annular disks of variable thickness, *International Journal for Computational Methods in Engineering Science and Mechanics*, **7**, 1-11

4. ALLAM M.N.M., ZENKOUR A.M., EL-AZAB T.M.A., 2007, Viscoelastic deformation of the rotating inhomogeneous variable thickness solid and annular disks, *International Journal for Computational Methods in Engineering Science and Mechanics*, **8**, 5, 313-322

5. ARGESO H., 2012, Analytical solutions to variable thickness and variable material property rotating disks for a new three-parameter variation function, *Mechanics Based Design of Structures and Machines*, **40**, 2, 133-152

6. ARNAB B., ISLAM S.M.R., KAHLAK A.A., AFSAR A.M., 2014, Finite difference solution to thermoelastic field in a thin circular FGM disk with a concentric hole, *Procedia Engineering*, **90**, 193-198

7. ASGHARI M., GHAFOORI E., 2010, A three-dimensional elasticity solution for functionally graded rotating disks, *Composite Structures*, **92**, 1092-1099

8. BAYAT M., SAHARI B.B., SALEEM M., ALI A., WONG S.V., 2009a, Bending analysis of a functionally graded rotating disk based on the first order shear deformation theory, *Applied Mathematical Modelling*, **33**, 4215-4230

9. BAYAT M., SAHARI B.B., SALEEM M., ALI A., WONG S.V., 2009b, Thermoelastic solution of a functionally graded variable thickness rotating disk with bending based on the first-order shear deformation theory, *Thin-Walled Structures*, **47**, 568-582

10. BAYAT M., SAHARI B.B., SALEEM M., HAMOUDA A.M.S., REDDY J.N., 2009c, Thermoelastic analysis of functionally graded rotating disks with temperature-dependent material properties: uniform and variable thickness, *International Journal of Mechanics and Material Design*, **5**, 263-279

11. BAYAT M., SALEEM M., SAHARI B.B., HAMOUDA A.M.S., MAHDI E., 2008, Analysis of functionally graded rotating disks with variable thickness, *Mechanics Research Communications*, **35**, 283-309

12. CAVALLARO L., 1965, Stress analysis of rotating disks, *Nuclear Structural Engineering*, **2**, 271-281

13. DAI H.-L., ZHENG, Z.-Q., DAI T., 2017, Investigation on a rotating FGPM circular disk under a coupled hygrothermal field, *Applied Mathematical Modelling*, **46**, 28-47

14. DAI T., DAI H.-L., 2015, Investigation of mechanical behavior for a rotating FGM circular disk with a variable angular speed, *Journal of Mechanical Science and Technology*, **29**, 9, 3779-3787

15. DAI T., DAI H.-L., 2017, Analysis of a rotating FGMEE circular disk with variable thickness under thermal environment, *Applied Mathematical Modelling*, **45**, 900-924

16. DAS D., SAHOO P., SAHA K., 2012, Dynamic analysis of rotating annular disk of variable thickness under uniform axial pressure, *International Journal for Computational Methods in Engineering Science and Mechanics*, **13**, 1, 37-59

17. ENTEZARI A., FILIPPI M., CARRERA E., 2017, On dynamic analysis of variable thickness disks and complex rotors subjected to thermal and mechanical prestresses, *Journal of Sound and Vibration*, **405**, 68-85

18. ENTEZARI A., KOUCHAKZADEH M.A., CARRERA E., FILIPPI M., 2017, A refined finite element method for stress analysis of rotors and rotating disks with variable thickness, *Acta Mechanica*, **228**, 575-594

19. ESSA S., ARGESO H., 2017, Elastic analysis of variable profile and polar orthotropic FGM rotating disks for a variation function with three parameters, *Acta Mechanica*, **228**, 3877-3899

20. FENG W.W., 1985, On finite deformation of viscoelastic rotating disks, *International Journal of Nonlinear Mechanics*, **20**, 1, 21-26

21. GHORBANPOUR ARANI A., KHODDAMI MARAGHI Z., MOZDIANFARD M.R., SHAJARI A.R., 2010a, Thermo-piezo-magneto-mechanical stresses analysis of FGPM hollow rotating thin disk, *International Journal of Mechanics and Material Design*, **6**, 341-349

22. GHORBANPOUR ARANI A., LOGHMAN A., SHAJARI A.R., AMIR S., 2010b, Semi-analytical solution of magneto-thermo-elastic stresses for functionally graded variable thickness rotating disks, *Journal of Mechanical Science and Technology*, **24**, 10, 2107-2117

23. GOLMAKANI M.E., 2013, Large deflection thermoelastic analysis of shear deformable functionally graded variable thickness rotating disk, *Composites: Part B*, **45**, 1143-1155

24. HARTOG D., 1952, *Advanced Strength of Materials*, New York, McGraw-Hill

25. HASSANI A., HOJJATI M.H., FARRAHI G., ALASHTI R.A., 2011, Semi-exact elastic solutions for thermo-mechanical analysis of functionally graded rotating disks, *Composite Structures*, **93**, 3239-3251

26. HASSANI A., HOJJATI M.H., MAHDAVI E., ALASHTI R.A., FARRAHI G., 2012, Thermo--mechanical analysis of rotating disks with non-uniform thickness and material properties, *International Journal of Pressure Vessels and Piping*, **98**, 95-101

27. HOSSEINI M., SHISHESAZ M., TAHAN K.N., HADI A., 2016, Stress analysis of rotating nano-disks of variable thickness made of functionally graded materials, *International Journal of Engineering Science*, **109**, 29-53

28. KADKHODAYAN M., GOLMAKANI M.E., 2014, Non-linear bending analysis of shear deformable functionally graded rotating disk, *International Journal of Non-Linear Mechanics*, **58**, 41-56

29. LEU S.-Y., CHIEN L.-C., 2015, Thermoelastic analysis of functionally graded rotating disks with variable thickness involving non-uniform heat source, *Journal of Thermal Stresses*, **38**, 415-426

30. MASHAT D.S., ZENKOUR A.M., 2014, Hygrothermal bending analysis of a sector-shaped annular plate with variable radial thickness, *Composite Structures*, **113**, 446-458

31. MURTHY D.N.S., SHERBOURNE A.N., 1970, Elastic stresses in anisotropic disks of variable thickness, *International Journal of Mechanical Sciences*, **12**, 827-640

32. PENG X.-L., LI X.-F., 2012, Elastic analysis of rotating functionally graded polar orthotropic disks, *International Journal of Mechanical Sciences*, **60**, 84-91

33. PENG X-L., LI X-F., 2012, Effects of gradient on stress distribution in rotating functionally graded solid disks, *Journal of Mechanical Science and Technology*, **26**, 1483-1492

34. RUHI M., ANGOSHTARI A., NAGHDABADI, R., 2005, Thermoelastic analysis of thick-walled finite--length cylinders of functionally graded materials, *Journal of Thermal Stresses*, **28**, 391-408

35. SAHNI M., SAHNI R., 2015, Rotating functionally graded disc with variable thickness profile and external pressure, *Procedia Computer Science*, **57**, 1249-1254

36. SHARMA J.N., SHARMA D., KUMAR S., 2013, Vibration analysis of a rotating FGM thermoelastic axisymmetric circular disk using FEM, *International Journal for Computational Methods in Engineering Science and Mechanics*, **14**, 262-270

37. SHERBOURNE A.N., MURTHY D.N.S., 1974, Stresses in disks with variable profile, *International Journal of Mechanical Sciences*, **16**, 449-459

38. TUTUNCU N., TEMEL B., 2013, An efficient unified method for thermoelastic analysis of functionally graded rotating disks of variable thickness, *Mechanics of Advanced Materials and Structures*, **20**, 38-46

39. VULLO V., VIVIO, F., 2008, Elastic stress analysis of non-linear variable thickness rotating disks subjected to thermal load and having variable density along the radius, *International Journal of Solids and Structures*, **45**, 5337-5355

40. WU N.-G., RAMSEY J.H., 1966, Stresses in a layered rotating disk, *International Journal of Mechanical Sciences*, **8**, 629-639

41. YELLA REDDY T., SRINATH H., 1974, Elastic stresses in a rotating anisotropic annular disk of variable thickness and variable density, *International Journal of Mechanical Sciences*, **16**, 85-89

42. YOU L.H., YOU X.Y., ZHANG J.J., LI J., 2007, On rotating circular disks with varying material properties, *Zeitschrift für angewandte Mathematik und Physik*, **58**, 1068-1084

43. ZAFARMAND H., HASSANI B., 2014, Analysis of two-dimensional functionally graded rotating thick disks with variable thickness, *Acta Mechanica*, **225**, 453-464

44. Zenkour A.M., 2005, Analytical solution for rotating exponentially-graded annular disks with various boundary conditions, *International Journal of Structural Stability and Dynamics*, **5**, 557-577

45. Zenkour A.M., 2009, Stress distribution in rotating composite structures of functionally graded solid disks, *Journal of Materials Processing Technology*, **209**, 3511-3517

46. Zenkour A.M., 2014, On the magneto-thermo-elastic responses of FG annular sandwich disks, *International Journal of Engineering Science*, **75**, 54-66

47. Zenkour A.M., Allam, M.N.M., 2006, On the rotating fiber-reinforced viscoelastic composite solid and annular disks of variable thickness, *International Journal for Computational Methods in Engineering Science and Mechanics*, **7**, 21-31

48. Zhenga Y., Bahalooa H., Mousanezhada D., Mahdib E., Vaziria A., Nayeb-Hashemi, H., 2016, Stress analysis in functionally graded rotating disks with non-uniform thickness and variable angular velocity, *International Journal of Mechanical Sciences*, **119**, 283-293